Polarized Light Monte Carlo Analysis of Birefringence-Induced Depolarization in Biological Tissues

Noé Ortega-Quijano, Félix Fanjul-Vélez, Irene Salas-García, José Luis Arce-Diego
Applied Optical Techniques Group, Electronics Technology, Systems and Automation Engineering Department, University of Cantabria, Avenida de los Castros S/N, 39005 Santander, Spain
ortegan@unican.es; arcedj@unican.es

ABSTRACT

In this work we analyze the impact of linear birefringence on biological tissues depolarization, which is essential for correctly interpreting experimental results. Our approach is based on the polarized light Monte Carlo method in transmission. We present a comparative analysis of light depolarization in biological tissues with different values of linear birefringence and particle sizes, in order to evaluate its impact on the calculated parameters.

Keywords: Polarized light propagation, anisotropic biological tissues, Monte Carlo, depolarization, birefringence.

1. INTRODUCTION

The application of optical techniques for non-invasive medical imaging is receiving a growing interest during the last decades [1]. The use of polarimetric techniques for biological tissues characterization has significant potential for diagnostic purposes, as it provides additional contrast mechanisms [2]. In this context, Mueller matrix polarimetry has become the main technique for characterizing the polarimetric properties of biological tissues [3].

Light propagation in biological tissues is dominated by multiple scattering, that arises from the high heterogeneity shown by tissues at the microscopic scale. The most relevant scattering particles are cell nuclei, cellular organelles like mitochondria, lisosomes and peroxisomes, and collagen fibers and fibrils [1,2]. Depolarization measured by Mueller matrix polarimetry depends both on the detection scheme and on the scattering particles characteristics (namely size, shape, concentration and optical contrast). The fact that many pathological processes provoke changes in the scattering particles enables to use depolarization as a diagnostic parameter [3,4].

Most biological tissues are anisotropic [2]. In particular, the main anisotropic property shown by biological tissues is linear birefringence. Other remarkable effects are optical activity and linear dichroism. It has been shown that the presence and variations of anisotropy in tissues can significantly modify depolarization [5,6]. Pathological processes usually modify anisotropic elements as well as scattering particles. Consequently, the observed depolarization is affected by both aspects, and therefore it is essential to understand the way in which birefringence and depolarization are interrelated in order to appropriately interpret depolarization parameters. However, this aspect has not been analyzed in detail so far.

In this work we present a numerical analysis of light depolarization in biological tissues with different values of linear birefringence, in order to evaluate its impact on the calculated parameters. Our approach is based on the polarized light Monte Carlo method for modeling light propagation in tissue-like optical media. We have developed our own code, which is based on an existing method [4,7] to which we have added anisotropic effects by using the differential Mueller matrix formalism [8-12].

Firstly, we present the Mueller calculus in Section 2, as well as the depolarization metrics that are used in this work. Then, differential Mueller matrix is introduced in Section 3, before summarizing the main steps of the polarized light Monte Carlo method in Section 4. Results are presented in Section 5, and Sections 6 includes the conclusions of this work.

Medical Laser Applications and Laser-Tissue Interactions VI, edited by Lothar D. Lilge, Ronald Sroka,
Proc. of OSA Biomedical Optics-SPIE Vol. 8803, 88030T · © 2013 OSA-SPIE
CCC code: 1605-7422/13/$18 · doi: 10.1117/12.2032169

2. MUELLER CALCULUS AND DEPOLARIZATION METRICS

Mueller calculus is a widely used matricial method that enables to fully characterize polarized light and its interaction with material media [13]. In this formalism, polarized light is represented by the Stokes vector $\vec{\mathbf{I}}$, which is directly related to the electric field components by:

$$\vec{\mathbf{I}} = \begin{bmatrix} I \\ Q \\ U \\ V \end{bmatrix} = \begin{bmatrix} \langle E_x E_x^* + E_y E_y^* \rangle \\ \langle E_x E_x^* - E_y E_y^* \rangle \\ \langle E_x E_y^* + E_y E_x^* \rangle \\ i\langle E_x E_y^* - E_y E_x^* \rangle \end{bmatrix}, \tag{1}$$

where E_x and E_y are the complex amplitudes of the beam, and the brackets denote the time averaging operation for the measurement period [13]. The first Stokes parameter (I) corresponds to the irradiance of the beam, and the remaining parameters are the differences between the intensity of horizontally and vertically polarized light (Q), +45º and −45º linearly polarized light (U), and right and left circularly polarized light (V). The total degree of polarization of a beam is defined as:

$$DOP = \frac{\left(Q^2 + U^2 + V^2\right)^{1/2}}{I}, \tag{2}$$

which equals 1 for totally polarized light, 0 for unpolarized light, and intermediate values for partially polarized light.

The polarimetric behavior of a linear sample is characterized by the Mueller matrix $\mathbf{M}$, a 4×4 real-element matrix that establishes the linear relationship between the input and output Stokes vectors:

$$\vec{\mathbf{I}}_{\mathbf{out}} = \mathbf{M}\vec{\mathbf{I}}_{\mathbf{in}}. \tag{3}$$

In general, $\mathbf{M}$ can alter the degree of polarization of the beam. In particular, for depolarizing media $DOP\left(\vec{\mathbf{I}}_{\mathbf{out}}\right) < DOP\left(\vec{\mathbf{I}}_{\mathbf{in}}\right)$. Biological tissues are one of the most preeminent examples of turbid media, which strongly depolarize light beams due to their microstructural heterogeneities.

It is of great interest to describe the depolarizing behavior of a sample by a single metric. There is a remarkable number of depolarization metrics, each of them based on a particular physical and mathematical approach. A first distinction can be established between direct and indirect depolarization metrics, depending on whether depolarization is directly quantified from the Mueller matrix or not. Among the direct depolarization metrics, the most popular ones are the depolarization index [14] and the average degree of polarization [15]. On the other side, indirect metrics make use of an intermediate step before quantifying depolarization. Cloude entropy [16] is based on the Mueller matrix Cloude decomposition, depolarization power is associated to the polar decomposition [17], and Lorentz depolarization indices are obtained through the symmetric decomposition [18]. In this work we will consider the depolarization index and the Cloude entropy.

Depolarization index DI quantifies the normalized Euclidean distance between the ideal depolarizer and the considered Mueller matrix [14]. This index can be directly obtained from the Mueller matrix by:

$$DI = \left[\frac{\mathrm{tr}\left(\mathbf{M}^{\mathrm{T}}\mathbf{M}\right) - M_{11}^2}{3M_{11}^2}\right]^{1/2}, \tag{4}$$

where M_{11} is the first Mueller matrix element. Depolarization index is 0 for a totally depolarizing Mueller matrix.

The parameter used for characterizing depolarization is the Cloude entropy, which requires first to calculate the covariance matrix $\mathbf{C}$ from the Mueller matrix $\mathbf{M}$ [16]. Covariance matrix is given by:

$$\mathbf{C} = \sum_{i,j=1}^{4} \mathbf{M_{ij}} \left(\boldsymbol{\sigma}_\mathbf{i} \otimes \boldsymbol{\sigma}_\mathbf{j}^{*} \right), \tag{5}$$

where * denotes the complex conjugate, $\otimes$ is the Kronecker product, and $\boldsymbol{\sigma}_\mathbf{i}$ are the well-known Pauli spin matrices [13]. Cloude entropy H is subsequently defined as:

$$H = \sum_{i=1}^{4} x_i \log_4 x_i \quad , \quad x_i = \lambda_{Ci} \Big/ \sum_{j=1}^{4} \lambda_{Ci} \, . \tag{6}$$

where λ_{Ci} are the eigenvalues of the covariance matrix. Cloude entropy ranges from 0 (non depolarizing sample) to 1 (completely depolarizing sample).

3. DIFFERENTIAL MUELLER MATRIX

Mueller calculus is suited to elements whose effect on the light beam takes place as an input-output mechanism. However, it does not enable to analyze the beam propagation through the sample. In that case, it is necessary to use the differential Mueller matrix.

The propagation of the Stokes vector $\vec{\mathbf{I}}$ through an optical medium along the z axis can be expressed as:

$$\frac{d\vec{\mathbf{I}}}{dz} = \mathbf{m}\vec{\mathbf{I}} \, , \tag{7}$$

being $\mathbf{m}$ the differential Mueller matrix that completely characterizes the polarimetric properties of an infinitesimal slab of the medium [9-12]. If homogeneity is assumed, the Mueller matrix and the differential Mueller matrix are related by:

$$\mathbf{M} = \exp\left(\mathbf{m}z\right), \tag{8}$$

where the matrix exponential is mathematically defined as the matrix with the same eigenvectors, whose eigenvalues are the exponential of the original matrix ones [9,10]. In previous works, it has been shown that if we assume that the beam always travels towards the observer in a right-handed Cartesian system, and the sign convention for the electric field vector is $\exp\left(ikz - i\omega t\right)$, where the complex propagation constant is $k = \eta + i\kappa$, the propagation constant η and the attenuation constant κ, the differential Mueller matrix for anisotropic depolarizing media [9] can be expressed as:

$$\mathbf{m} = \begin{bmatrix} -\mu_e & \kappa_q + \kappa_q^{'} & \kappa_u + \kappa_u^{'} & \kappa_v + \kappa_v^{'} \\ \kappa_q - \kappa_q^{'} & -\mu_e - \mu_q^{'} & \eta_v + \eta_v^{'} & -\eta_u - \eta_u^{'} \\ \kappa_u - \kappa_u^{'} & -\eta_v + \eta_v^{'} & -\mu_e - \mu_u^{'} & \eta_q + \eta_q^{'} \\ \kappa_v - \kappa_v^{'} & \eta_u - \eta_u^{'} & -\eta_q + \eta_q^{'} & -\mu_e - \mu_v^{'} \end{bmatrix}, \tag{9}$$

It can be observed that this equation involves a total of 16 differential parameters that quantify the full set of elementary optical properties of the sample, including the non-depolarizing and depolarizing ones. The differential parameters for birefringence and dichroism are related to the complex propagation constant by $\eta_{q,u,v} = \eta_{y,-45^\circ,lcp} - \eta_{x,+45^\circ,rcp}$ and $\kappa_{q,u,v} = \kappa_{y,-45^\circ,lcp} - \kappa_{x,+45^\circ,rcp}$, where the subscripts indicate the direction to be considered in each case. In Table 1, the non-depolarizing parameters and the description of its physical significance have been included for the sake of clarity.

4. POLARIZED LIGHT MONTE CARLO METHOD

Monte Carlo method is a widely used approach for modeling light propagation in biological tissues. It constitutes a stochastic method for statistically solving photon propagation in samples where scattering dominates over absorption (i.e. turbid media). The method relies on the determination of several probability distributions based on a comprehensive model of light propagation in turbid media [19]. Due to the statistical nature of the method, a larger number of photons implies a better accuracy of the results obtained. In this work, our code is written in Matlab and is based in the polarized light Monte Carlo method described in [20].

Table 1. Non-depolarizing differential parameters and description of the properties characterized by each of them.

Parameter	Property
μ_e	Isotropic extinction
κ_q	Linear dichroism along $x-y$
κ_u	Linear dichroism along $\pm 45^\circ$
κ_v	Circular dichroism
η_q	Linear birefringence along $x-y$
η_u	Linear birefringence along $\pm 45^\circ$
η_v	Circular birefringence

The first step of the method is launching a packet of photons, which is initially given a weight $W=1$, a position $\vec{\mathbf{r}}$, and a propagation direction $\hat{\mathbf{n}}=\begin{pmatrix} n_x & n_y & n_z \end{pmatrix}$. Additionally, an auxiliary vector $\hat{\mathbf{v}}$ is fixed in order to keep track of the meridional reference plane. The state of polarization of the photon packet is characterized by its Stokes vector $\vec{\mathbf{I}}$. The photon displacement Δs is calculated for each step by:

$$\Delta s = \frac{-\ln\left(\xi_1\right)}{\mu_e}, \tag{10}$$

where μ_e is the extinction coefficient of the medium, and $\xi_1 \in (0,1]$ is a pseudo-random number. The new position of the photon packet is obtained directly from the displacement and the unitary propagation vector:

$$\vec{r}' = \vec{r} + \Delta s \cdot \hat{n}. \tag{11}$$

The effect of absorption in each displacement step is modeled by the following reduction in the packet weight:

$$\Delta W = \frac{\mu_a}{\mu_e} W. \tag{12}$$

Apart from absorption, the effect of anisotropy on the Stokes vector must be included at this step. Anisotropy is modeled by a macroscopic Mueller matrix $\mathbf{M}\big|_{\Delta s,\hat{\mathbf{n}}}$ that depends on both photon displacement and the relative orientation of the photon packet meridional plane with respect to the anisotropic fast axis. In this work, we obtain the differential Mueller matrix and then obtain the macroscopic Mueller matrix. This approach has the advantage that can be further applied to samples with simultaneous coupled effects. The new Stokes vector is calculated as:

$$\vec{\mathbf{I}}' = \mathbf{M}\big|_{\Delta s,\hat{\mathbf{n}}}\, \vec{\mathbf{I}}. \tag{13}$$

The statistical sampling implemented in the displacement calculation implies that, if the photon continues in the medium, a scattering event takes place. The essential aspect in this step is to calculate the scattering angle Θ and the rotation angle Θ^{rot} in the scattering plane [20], that modify its propagation direction as a result of the elastic electromagnetic interaction of the photon packet with the scattering particle. Scattering phase function is expressed by the following equation:

$$p\left(\Theta,\Theta^{rot},\vec{\mathbf{S}}\right) = F_{11}(\Theta) I + F_{12}(\Theta)\left[Q\cos\left(2\Theta^{rot}\right) + U\sin\left(2\Theta^{rot}\right)\right], \tag{14}$$

where F_{11} and F_{12} are elements of the 4×4 scattering matrix given by Mie theory if the scatterers are spherical. g is the scattering anisotropy [3]. Angles Θ and Θ^{rot} are calculated by the rejection method [20].

Scattering matrix is defined in the scattering plane. Therefore, it is necessary to perform a transformation of the Stokes vector from the meridional plane to the scattering plane while carrying the information of the photon packet reference

system. In the polarized light Monte Carlo method based on quaternions, the new reference system is obtained by two consecutive rotations implemented by quaternions products. The first rotation is:

$$\hat{\mathbf{v}}' = \mathbf{q}^{*}_{\Theta^{\mathrm{rot}}} \hat{\mathbf{v}} \mathbf{q}_{\Theta^{\mathrm{rot}}} , \tag{15}$$

where

$$\mathbf{q}_{\Theta^{\mathrm{rot}}} = \cos\left(\Theta^{rot}/2\right) + \hat{\mathbf{i}} n_x \sin\left(\Theta^{rot}/2\right) + \hat{\mathbf{j}} n_y \sin\left(\Theta^{rot}/2\right) + \hat{\mathbf{k}} n_z \sin\left(\Theta^{rot}/2\right), \tag{16}$$

and the second one is

$$\hat{\mathbf{n}}' = \mathbf{q}^{*}_{\Theta} \hat{\mathbf{n}} \mathbf{q}_{\Theta} , \tag{17}$$

where

$$\mathbf{q}_{\Theta} = \Theta + \hat{\mathbf{i}} v_x + \hat{\mathbf{j}} v_y + \hat{\mathbf{k}} v_z , \tag{18}$$

Finally, the Stokes vector resulting from the scattering event can be obtained by the following expression:

$$\vec{\mathbf{I}}' = \mathbf{F}(\Theta) \mathbf{M}_{\ominus} \left(\Theta^{rot}\right) \vec{\mathbf{I}} , \tag{19}$$

where $\mathbf{M}_{\ominus}$ is the rotation matrix for angle Θ and $\mathbf{F}(\Theta)$ is the scattering matrix for such angle .

The transport of the photon packet finishes when it is absorbed or transmitted/backscattered. The last step is to perform to consecutive rotations. The first rotation angle α_1^d is given by:

$$\alpha_1^d = \begin{cases} 0 \text{ , if } n_z = v_z = 0 \\ \tan^{-1}\left(-v_z / w_z\right) \text{ , rest} \end{cases}, \tag{20}$$

where is the third component of vector $\hat{\mathbf{w}} = \hat{\mathbf{v}} \times \hat{\mathbf{n}}$. The second rotation angle α_2^d is

$$\alpha_2^d = \begin{cases} \tan^{-1}\left(n_y / n_x\right) \text{ , transmitted} \\ -\tan^{-1}\left(n_y / n_x\right) \text{ , backscattered} \end{cases}, \tag{21}$$

Finally, the detected Stokes vector is:

$$\vec{\mathbf{I}}^{\mathbf{det}} = \mathbf{M}_{\ominus}\left(\alpha_2^d\right) \mathbf{M}_{\ominus}\left(\alpha_1^d\right) \Lambda^n \vec{\mathbf{I}} , \tag{22}$$

where Λ is the medium albedo and n is the total number of number of scattering events.

5. RESULTS

In this work we have considered five different scattering particles which span the typical ranges observed in biological tissues. Their characteristics are summarized in Table 1. Scattering particles refractive index is 1.59 in all of them. Scattering parameters have been calculated using Mie theory (i.e. spherical scattering particles have been considered) [21]. It can be observed that the total scattering coefficient was roughly 64 cm^{-1} in all cases. The values of linear birefringence were varied from $\Delta n = 0$ to $2.8 \cdot 10^{-4}$, in steps of $4 \cdot 10^{-5}$, which lead to a total of an isotropic sample and seven different anisotropic samples for each scattering particle. Linear birefringence is parallel to the x axis. The medium refractive index is 1.34, and the fixed sample length is 0.1 cm. We have considered a wavelength of 632.8 nm for all the simulations, which corresponds to a HeNe laser. Detection has been modeled in transmission configuration with on-axis detection, sample-detector distance of 0.25 cm, detector area of 0.04 cm^2, and detection angle of 30 degrees. The number of photons used in each simulation was fixed in such a way that a minimum of 10^6 photons were detected in transmission.

Table 2. Characteristics of the scattering particles considered in the polarized light Monte Carlo model.

Particle diameter [µm]	Scattering cross section [µm^2]	Scattering anisotropy	Numerical density [particles/µm^3]	Scattering coefficient [mm^{-1}]
100	0.000053	0.076	1220	64.752
250	0.006430	0.502	10	64.305
500	0.139199	0.825	0.460	64.032
750	0.689679	0.896	0.094	64.485
1000	1.928060	0.920	0.034	64.590

The depolarization index calculated from the transmitted Mueller matrices obtained for all the modeled scenarios is presented in Figure 1. The results clearly show that birefringence effectively increases depolarization. It is interesting to note that the slope of the curves for each particle diameter is lower for small particles, and becomes more pronounced as the scattering particles diameter becomes larger. Apart from that, depolarization is obviously higher for small particles, i.e. depolarization observed in transmission is greater for scattering in the Rayleigh regime. Such characteristic arise from the scattering characteristics of small particles, which randomize photon trajectories in a stronger way with comparison to the largest particles considered in this work. This effect is closely related to the scattering anisotropy of the scattering particles (Table 1), which takes a value of 0 for isotropic scattering (which causes stronger randomization of photon trajectories and state of polarization) and a value of 1 for forward-directed scattering (resulting in a weaker randomization).

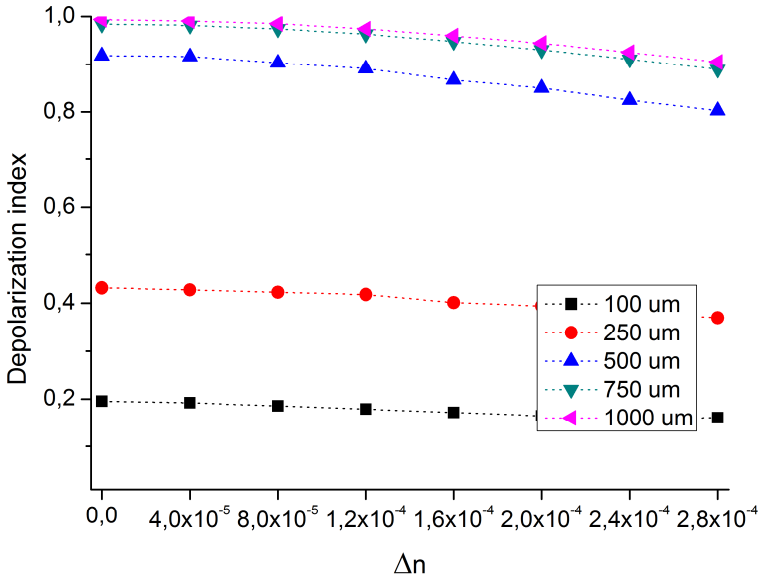

Fig. 1. Depolarization index as a function of linear birefringence for scattering particles with diameter of 100, 250, 500, 750 and 1000 µm.

Apart from the depolarization index, the Cloude entropy has also been calculated. The Cloude entropy values obtained for all the modeled scenarios are presented in Figure 2. The results complement those previously presented, and show the same trends. In this case, the results are presented in logarithmic scale, which enables to better appreciate the slopes of the Cloude entropy curves for large particles. The fact that both the depolarization index and the Cloude entropy show the same behavior proves that depolarization is a physical effect that takes place in the sample, and not an error due to calculations or incorrect assumptions.

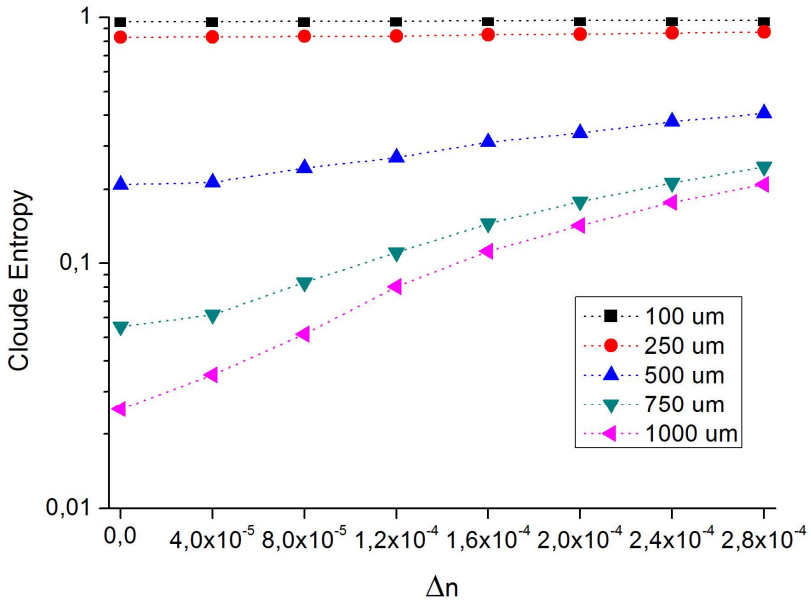

Fig. 2. Cloude entropy as a function of linear birefringence for scattering particles with diameter of 100, 250, 500, 750 and 1000 μm (note that the y-axis is plotted in logarithmic scale).

6. CONCLUSIONS

We have presented an application of the polarized light Monte Carlo method to the study of the interrelation between birefringence and depolarization in biological tissues. This work constitutes a first step towards an appropriate understanding of the impact of birefringence on depolarization, which is essential for correctly interpreting experimental results. Other aspects to be analyzed in future works include a similar study in backscattering configuration, as well as the proposal of methods to decouple birefringence-induced depolarization from the one exclusively produced by scattering particles.

REFERENCES

[1] Vo-Dinh, T., [Biomedical Photonics Handbook], CRC (2003).
[2] Tuchin, V. V., Wang, L. V. and Zimnyakov, D. A., [Optical Polarization in Biomedical Applications], Springer (2006).
[3] Ghosh, N. and Vitkin, I. A., "Tissue polarimetry: concepts, challenges, applications, and outlook," J. Biomed. Opt. 16, 1108011–11080129 (2011).
[4] Ortega-Quijano, N., Fanjul-Vélez, F., de Cos-Pérez, J. and Arce-Diego, J. L., "Analysis of the depolarizing properties of normal and adenomatous polyps in colon mucosa for the early diagnosis of precancerous lesions," Opt. Comm. 284, 4852–4856 (2011).
[5] Jacques, S. L., Ramella-Roman, J. C. and Lee, K., "Imaging skin pathology with polarized light," J. Biomed. Opt. 7, 329–340 (2002).
[6] Alali, S., Ahmad, M., Kim, A., Vurgun, N., Wood, M. F. G. and Vitkin, I. A., "Quantitative correlation between light depolarization and transport albedo of various porcine tissues," J. Biomed. Opt. 17, 0450041–0450048 (2012).
[7] Ramella-Roman, J. C., Prahl, S. A. and Jacques, S. L., "Three Monte Carlo programs of polarized light transport into scattering media: part I," Opt. Express 13, 4420–4438 (2005).
[8] Azzam, R. M. A., "Propagation of partially polarized light through anisotropic media with or without depolarization: A differential 4 × 4 matrix calculus," J. Opt. Soc. Am. 68, 1756–1767 (1978).
[9] Ortega-Quijano, N. and Arce-Diego, J. L., "Depolarizing differential Mueller matrices," Opt. Lett. 36, 2429–2431 (2011).

[10] Ortega-Quijano, N. and Arce-Diego, J. L., "Mueller matrix differential decomposition," Opt. Lett. 36, 1942–1944 (2011).
[11] Ortega-Quijano, N. and Arce-Diego, J. L., "Mueller matrix differential decomposition for direction reversal: application to samples measured in reflection and backscattering," Opt. Express 19, 14348–14353 (2011).
[12] Ortega-Quijano, N., Haj-Ibrahim, B., García-Caurel, E., Arce-Diego, J. L. and Ossikovski, R., "Experimental validation of Mueller matrix differential decomposition," Opt. Express 20, 1151–1163 (2012).
[13] Brosseau, C., [Fundamentals of polarized light], Wiley, (1998).
[14] Gil, J. J. and Bernabeu, E., "A depolarization criterion in Mueller matrices," Opt. Acta 32, 259–261 (1985).
[15] Chipman, R. A., "Depolarization index and the average degree of polarization," Appl. Opt. 44, 2490–2495 (2005).
[16] Cloude, S. R., "Group theory and polarisation algebra," Optik 75, 26–36 (1986).
[17] Lu, S. Y. and Chipman, R. A., "Interpretation of Mueller matrices based on polar decomposition," J. Opt. Soc. Am. A 13, 1106–1113 (1996).
[18] Ossikovski, R., "Alternative depolarization criteria for Mueller matrices," J. Opt. Soc. Am. A 27, 808–814 (2010).
[19] Wang, L. V., Wu, W., [Biomedical Optics. Principles and Imaging], Wiley (2007).
[20] Ramella-Roman, J. C., Prahl, S. A., and Jacques, S. L., "Three Monte Carlo programs of polarized light transport into scattering media: part I," Opt. Express 13, 4420–4438 (2005).
[21] Bohren, C. F. and Huffman, D. R., [Absorption and Scattering of Light by Small Particles], Wiley (1998).